Protein Kinase A-Mediated Effects of Protein Kinase C Partial Agonist 5-(Hydroxymethyl)Isophthalate 1a3 in Colorectal Cancer Cells

Tarvainen, Ilari

2022-01-01

http://hdl.handle.net/10138/350100
https://doi.org/10.1124/jpet.121.000848

unspecified
acceptedVersion
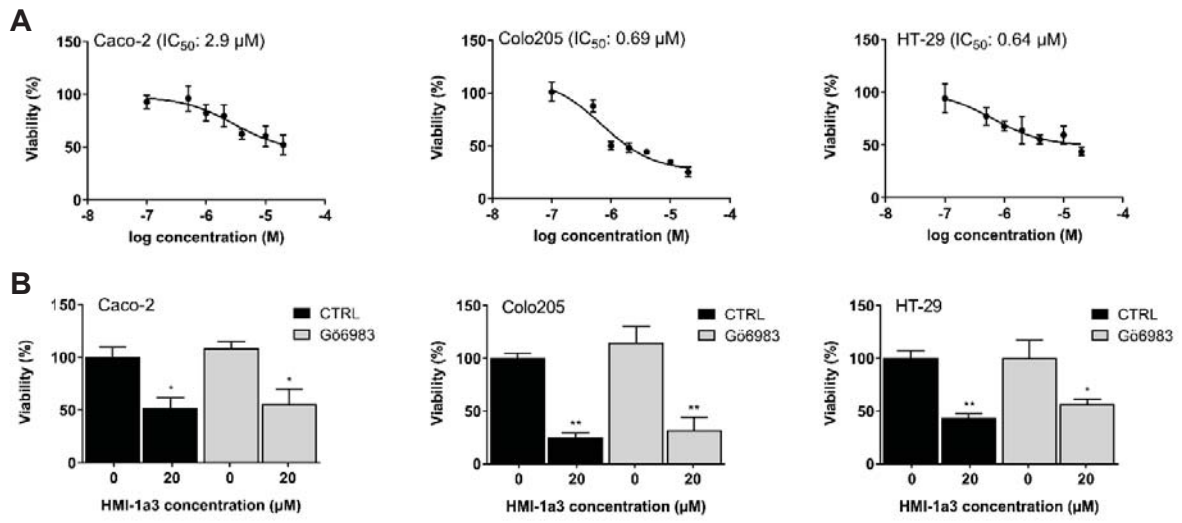
Figure 1.

Figure 2.
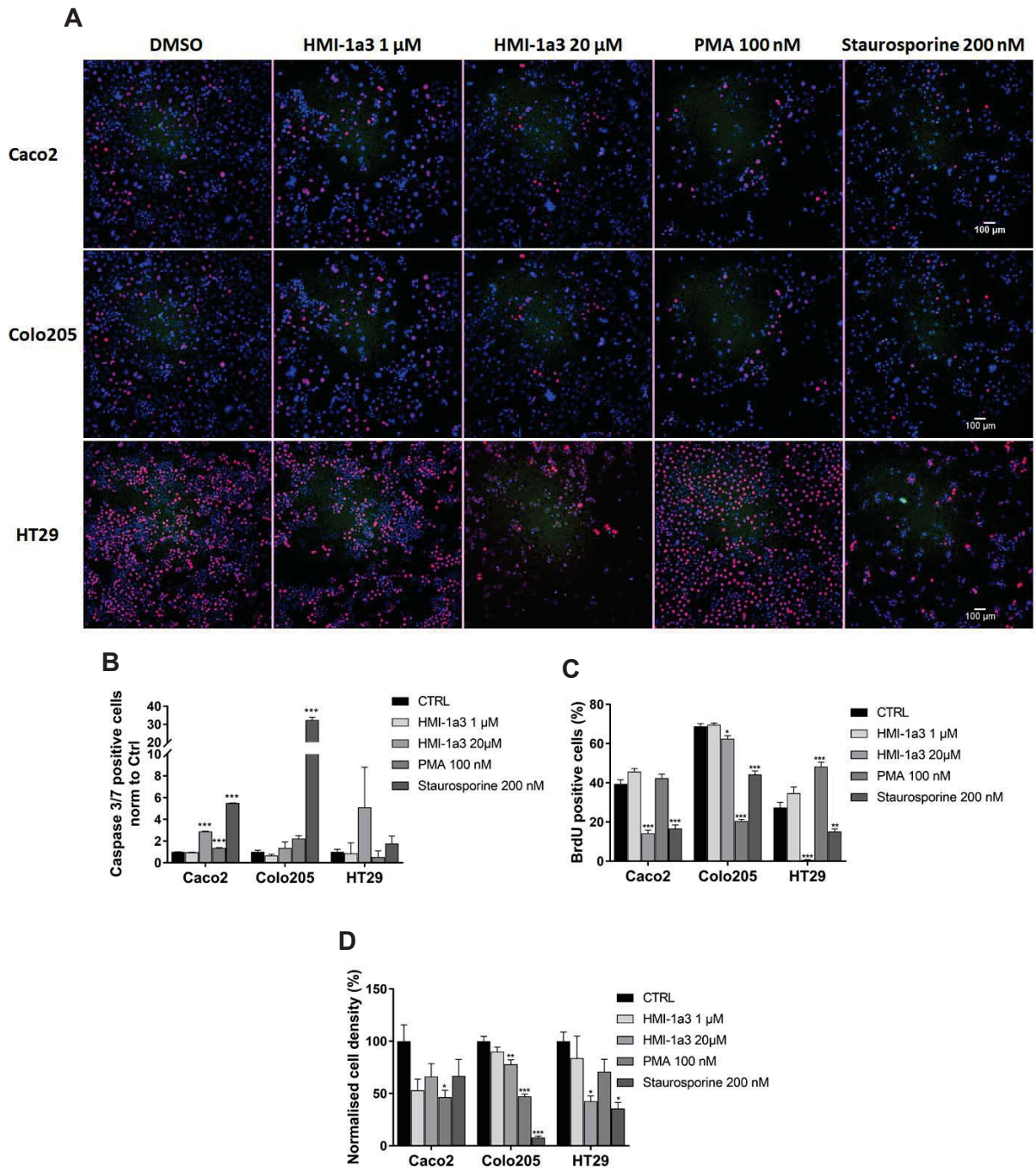
Figure 3.
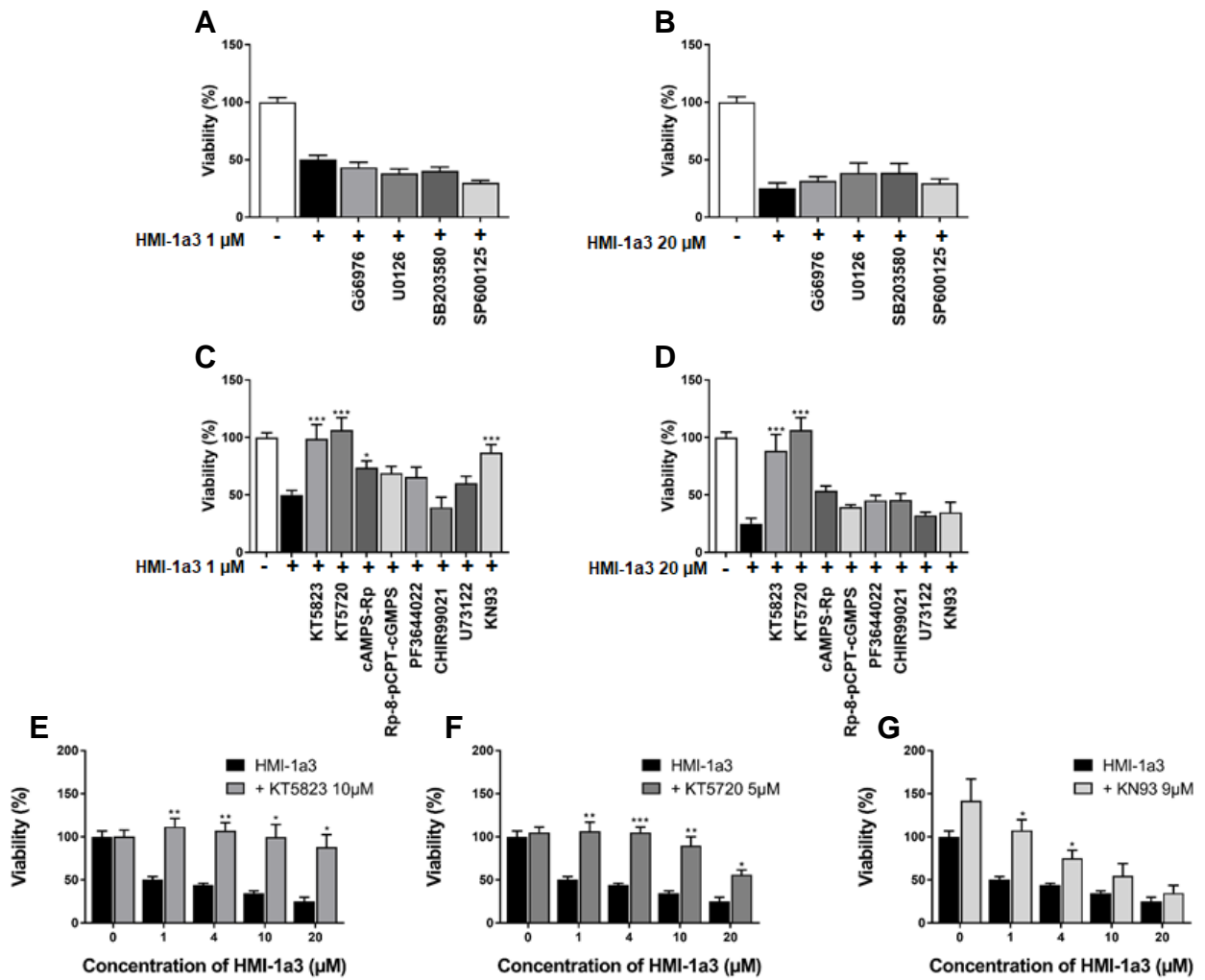
Figure 4.

A
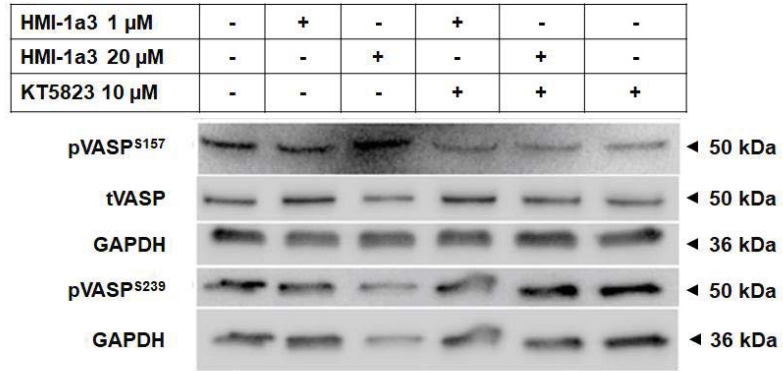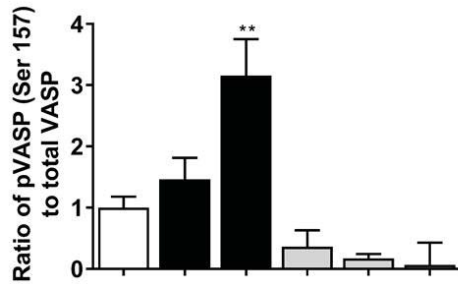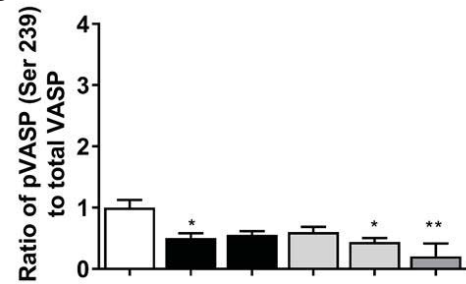
HMI-1a3 1 µM	-	+	-	+	-	-
HMI-1a3 20 µM	-	-	+	-	+	-
KT5823 10 µM	-	-	-	+	+	+

pVASP^{S157} ◄ 50 kDa

tVASP ◄ 50 kDa

GAPDH ◄ 36 kDa

pVASP^{S239} ◄ 50 kDa

GAPDH ◄ 36 kDa

B

Ratio of pVASP (Ser 157) to total VASP

HMI-1a3 1 µM	-	+	-	+	-	-
HMI-1a3 20 µM	-	-	+	-	+	-
KT5823 10 µM	-	-	-	+	+	+

C

Ratio of pVASP (Ser 239) to total VASP

HMI-1a3 1 µM	-	+	-	+	-	-
HMI-1a3 20 µM	-	-	+	-	+	-
KT5823 10 µM	-	-	-	+	+	+

Figure 5.

Previously verified targets

β2-chimaerin

PKCδ   PKD1

PKCα   MRCKα

CF₃   CF₃

HMI-1a3

New target?

cAMP/PKA

Effects on colorectal cancer cell lines

Caco2
  ↓ Viability
  ↓ Proliferation
  ↑ Apoptosis

Colo205
  ↓ Viability
 ↓ Proliferation
 ↑ Apoptosis

HT29
  ↓ Viability
  ↓ Proliferation
  ↑ Apoptosis
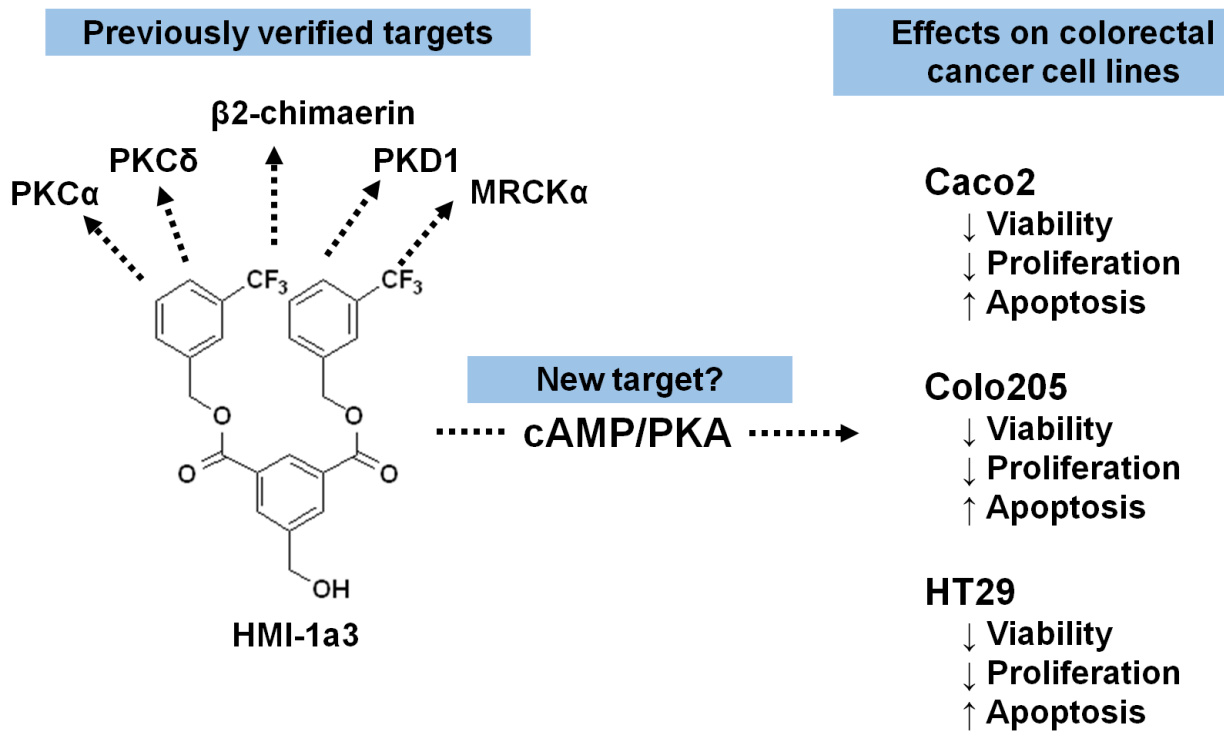
Protein kinase A Mediated Effects of Protein kinase C Partial Agonist HMI-1a3 in Colorectal Cancer Cells

Ilari Tarvainen*, Rebecca C. Nunn, Raimo K. Tuominen, Maria H. Jäntti, Virpi Talman

Affiliations

IT, RCN, RKT, MHJ and VT: Drug Research Program and Division of Pharmacology and Pharmacotherapy, Faculty of Pharmacy, University of Helsinki, Finland

*Corresponding author

Running title: PKA Mediated Effects of HMI-1a3 in Colorectal Cancer Cells

Corresponding author:

Ilari Tarvainen

Division of Pharmacology and Pharmacotherapy

Faculty of Pharmacy

University of Helsinki

P.O. Box 56 (Viikinkaari 5E)

FI-00014 Helsinki, FINLAND

Tel: +358504487245

Email: ilari.tarvainen@helsinki.fi

Number of text pages: 31

Number of tables: 2

Number of figures: 5

Number of references: 52

Number of words in the Abstract: 164

Number of words in the Introduction: 545

Number of words in the Discussion: 1050

Abbreviations: BrdU, 5-bromo-2'-deoxyuridine; cAMP, cyclic adenosine monophosphate; CRC, colorectal cancer; DAG, diacylglycerol; HCA, high-content analysis; LDH, lactate dehydrogenase; MTT, 3-(4,5-dimethylthiazol-2-yl)-2,5-diphenyltetrazolium bromide; PKA, protein kinase A; PKC, Protein kinase C

Abstract

Colorectal cancer is the third most commonly occurring cancer in men and the second in women. The global burden of colorectal cancer is projected to increase to over 2 million new cases with over 1 million deaths within the next 10 years and there is a great need for new compounds with novel mechanisms of action. Our group has developed PKC modulating isophthalic acid derivatives that induce cytotoxicity towards human cervical and prostate cancer cell lines. In this study, we investigated the effects of 5-(hydroxymethyl)isophthalate 1a3 (HMI-1a3) on colorectal cancer cell lines (Caco2, Colo205 and HT29). HMI-1a3 inhibited cell proliferation, decreased cell viability and induced an apoptotic response in all studied cell lines. These effects, however, were independent of PKC. Using serine/threonine kinome profiling and pharmacological kinase inhibitors we identified activation of the cAMP/PKA pathway as a new mechanism-of-action for HMI-1a3-induced anti-cancer activity in colorectal cancer cell lines. Our current results strengthen the hypothesis for HMI-1a3 as a potential anti-cancer agent against various malignancies.

Significance statement

Colorectal cancer (CRC) is a common solid organ malignancy. Here, we demonstrate that the protein kinase C (PKC) C1 domain-targeted isophthalatic acid derivative HMI-1a3 has anti-cancer activity on CRC cell lines independently of PKC. We identified protein kinase A (PKA) activation as a mechanism of HMI-1a3 induced anti-cancer effects. Our results reveal a new anti-cancer mechanism of action for the partial PKC agonist HMI-1a3 and thus provide new insights for the development of PKC and PKA modulators for cancer therapy.

Introduction

Worldwide, approximately 10 % of all diagnosed cancers and cancer-related deaths are due to colorectal cancer (CRC). (Bray et al., 2018). Although the prognosis of patients with CRC has improved during the past decades, the 5-year survival rate remains around 50% to 65% (Bray & Soerjomataram, 2015; Brenner et al., 2012). Therefore, new treatment regimens to combat advanced disease with alternative therapeutic strategies are needed.

Protein kinases play a key role in tumour growth and progression, thus they have been an attractive target for drug discovery for decades. As of August 20th 2021 the U.S. Food and Drug Administration (FDA) has approved 73 small molecules targeting protein kinases (Cohen et al., 2021; FDA, 2021). These compounds are mainly protein kinase inhibitors, as protein kinase cascades are frequently hyperactivated in cancer.

Majority of the drugs target either directly or allosterically the ATP binding site of a protein kinase (Roskoski, 2015). Since the ATP-binding site among various protein kinases shares structural similarity, most if not all protein kinase inhibitors inhibit several kinases at the same time. Even so, usually the therapeutic effect is remarkable. Targeting regulatory domain of intracellular protein kinases has been less studied, but we and others have demonstrated PKC-C1 domain as potential target (Bessa et al., 2018; Jäntti et al., 2018). Protein kinase A (PKA) and protein kinase C (PKC) are serine/threonine kinases involved in CRC development (Kisslov et al., 2012; Spindler et al., 2009). Several lines of evidence suggest that activation of PKA inhibits progression of CRC (Zhao et al., 2021). Investigational inhibitors of PKC targeting the ATP-binding site have failed in clinical trials for CRC (Ouaret & Larsen, 2014). In the case of PKC rather than inhibiting its activity, therapeutic strategies should aim to restore its activity (Antal et al., 2015). Among more than 500 PKC mutations in biopsies from cancer patients, detailed characterization of 46 representative mutations showed that cancer-associated point mutations in PKC were loss-of-function mutations. Similar results have been reported also by other research groups (Craven & DeRubertis, 1994; Dowling et al., 2016; Pongracz et al., 1995; Suga et al., 1998). These findings change

substantially the generally believed role of PKC in tumour promotion and progression (Gorin & Pan, 2009). Considering this, it seems reasonable that instead of inhibiting PKC we should aim at preserving or increasing its activity to treat cancer.

Our group has previously developed isophthalic acid derivatives binding to the C1-domain of classical and novel PKCs modulating their activity without inducing downregulation of PKC (Boije af Gennäs et al., 2009; Jäntti et al., 2018). They have been demonstrated to possess PKC mediated neuroprotective effects against neuroinflammation (Sarajärvi et al., 2018), and antifibrotic effects on cardiac fibroblasts (Karhu et al., 2021). They also inhibit the proliferation of HeLa human cervical cancer cells and induce senescence or apoptosis in PC3, DU145 and LNCaP prostate cancer cell lines (Jäntti et al., 2018; Talman et al., 2011). Since there is strong evidence suggesting that PKCs play tumour suppressing role especially in colorectal cancer (Antal et al., 2015; Choi et al., 1990; Dowling et al., 2016), yet the anticancer effects observed in the previous studies have not been fully PKC mediated, we aimed to unravel the effects and mechanisms of 5-(hydroxymethyl) isophthalate 1a3 (HMI-1a3) in colorectal cancer cell lines Caco-2, Colo205 and HT-29.

Materials and methods

Compounds and reagents

HMI-1a3 (bis(3-trifluoromethylbenzyl) 5-(hydroxymethyl)isophthalate) was synthesized at the Division of Pharmaceutical Chemistry and Technology, Faculty of Pharmacy, University of Helsinki, as described previously (Boije af Gennäs et al., 2009). HD NMR spectrometery (Bruker Ascend 400 MHz-Avance III, Bruker Corporation, Billerica, MA, USA) was used to verify the identity of the compounds. Exact mass and purity (>95%) of each batch was confirmed by LC-MS with a Waters Acquity® UPLC system (Waters, Milford, MA, USA) that was equipped with an Acquity UPLC® BEH C18 column (1.7 µm, 50 x 2.1 mm, Waters, Dublin, Ireland) and Acquity PDA detector. Waters Synapt G2 HDMS mass spectrometer (Waters, Milford, MA, USA) was used with an ESI ion source in positive mode. The PKC-activator phorbol 12-myristate 13-acetate (PMA), the pan-PKC inhibitor Gö6983, and the conventional-PKC inhibitor Gö6976, Glycogen synthase kinase 3 (GSK-3) inhibitor CHIR99021 were from Sigma-Aldrich (Steinheim, Germany). Ca2+/calmodulin-dependent protein kinase 2 (CaMK 2) inhibitor KN93, JNK inhibitor SP600125, MEK1/2 inhibitor U0126, MK2/PRAK inhibitor PF 3644022, p38α and p38β (MAPK) inhibitor SB203580, phospholipase C inhibitor U73122, PKA inhibitor KT5720, PKA inhibitor cAMPS-Rp, PKG inhibitor KT5823 and Staurosporine were from Tocris Bioscience (Bristol, UK).

Trans-Blot® Turbo™ Midi PVDF Transfer Packs and 12% Mini-Protean® TGX Stain-Free™ Protein Gels used for western blotting were purchased from Bio-Rad. The Pierce™ BCA Protein Assay Kit and SuperSignal™ West Femto Maximum Sensitivity Substrate reagents were from Thermo Scientific. Primary antibodies were acquired from the following sources: E2F1 (#3742, 1:2000, Cell Signaling Technology), p21 Waf1/Cip1 (#2946, 1:1000, Cell Signaling Technology), phospho-VASP (Ser 157) (# 365564, 1:200, Santa Cruz Biotechnology, Dallas, TX, USA), phospho-VASP (Ser 239) (# 3114, 1:1000, Cell Signaling Technology), cleaved PARP (#9541, 1:1000, Cell Signaling Technology, Danvers, MA, USA), VASP (#46668, 1:1000, Santa Cruz Biotechnology), anti-β-actin (#4967, 1:1000, Cell

Signaling Technology) and Anti-Glyceraldehyde-3-Phosphate Dehydrogenase Antibody, clone 6C5 (GAPDH) (MAB374, 1:10000, Sigma-Aldrich). The secondary horseradish peroxidase (HRP)-linked antibodies: goat anti-rabbit IgG (#7074; 1:2000) and horse anti-mouse IgG (#7076; 1:2000) were bought from Cell Signaling Technology.

For immunofluorescence staining and high content analysis (HCA), 5-Bromo-2'-deoxyuridine (BrdU) was acquired from Abcam (Cambridge, UK), monoclonal rat anti-BrdU (#ab6326) from Abcam and the Alexa Fluor 647-conjugated goat anti-rat IgG from Life Technologies (#A21247). The DNA stain 4',6-diamidino-2-phenylindole (DAPI) was from Sigma-Aldrich. CellEvent™ Caspase-3/7 Green Detection Reagent was purchased from Invitrogen (Carlsbad, CA, USA).

Cell culture

The human colorectal cancer cell lines: Caco-2 (Colorectal adenocarcinoma; male), Colo205 (Colorectal adenocarcinoma; male) and HT-29 (Colorectal adenocarcinoma; female) were purchased from the American Type Culture Collection (Manassas, VA, USA). Colo205 cells were cultured in RPMI1640 medium (Cat #1060120, MP Biomedicals, Santa Ana, CA, USA) and Caco-2 and HT-29 cells were cultured in Dulbecco's modified Eagle's medium (D-7777; Sigma-Aldrich). For all cell lines, the basal media were supplemented with 10% foetal bovine serum (FBS), 100 units/mL penicillin, and 100 µg/mL streptomycin (all sourced from Gibco). Cell cultures were maintained at 37 °C in a humidified atmosphere of 5% CO_2. For viability and high-content analysis (HCA) cells were plated on Corning Costar® 96-well plates, and for immunoblotting and Ser/Thr kinase profiling on plastic six-well plates.

Cell viability assays

Cell viability was determined by the MTT (3-(4,5-dimethylthiazol-2-yl)-2,5-diphenyltetrazolium bromide) reduction assay, and cell membrane integrity using lactate dehydrogenase (LDH) release assay from cell culture media, as previously described (Tarvainen et al., 2020). In brief, the cells seeded onto 96-well plates (10 000 cells per well, in serum-supplemented

media), were incubated with the compounds in normal cell culture medium for 24 h. The LDH assay was carried out with 50 µL samples of culture medium from each well. Fifty microliters of substrate solution was added and after a 30 min incubation at room temperature (RT) in the dark, the reaction was stopped by adding 50 µL of 1 M acetic acid. Absorbance was measured at 490 nm using Victor2 plate reader (PerkinElmer, Turku, Finland). Spontaneous, maximal and background LDH activity was quantified from cell culture medium of untreated cells, medium of cells lysed with 0.9% Triton X-100 and medium without cells, respectively. For quantification of metabolic activity, MTT solution was added to the cells at a final concentration of 0.5 mg/ mL, and the cells were grown for a further 2 h in cell culture conditions. The cell culture media was then aspirated and DMSO (200 µL) added to dissolve the formazan crystals. Absorbance was measured at 550 nm, subtracting absorbance at 650 nm as background. Experiments were performed in biological triplicates.

Immunoblotting

For the analysis of protein expression or phosphorylation, cells were plated at 4.0×10^5 cells/well on six-well plates and let to attach for 24 h. The cells were then exposed to the compounds (to study cleavedPARP, E2F1, p21 Waf1/Cip1), or the medium was changed to a serum-free cell culture medium for 24 h prior to the compound exposure (to study vasodilator-stimulated phosphoprotein (VASP)). The cells were treated with the test compounds for the indicated times, after which the medium was removed and the cells were washed twice with ice-cold phosphate-buffered saline (PBS). Cells were then harvested in ice-cold lysis buffer containing 1 mM ethylenediaminetetraacetic acid (EDTA), 150 mM NaCl, 0.25% NP-40, 1% Triton X-100, 10 mM Tris-HCl, pH 6.8) supplemented with Complete protease inhibitors (Roche, Mannheim, Germany) and PHOStop phosphatase inhibitors (Roche, Mannheim, Germany). Cell homogenates were centrifuged at 13,000 g for 4 min at 4 °C and the supernatants collected for further analysis. Protein concentrations were determined with bicinchoninic acid protein assay kit. Equal amounts of protein (10 µg per lane) were resolved on a 12% Mini-protean TGX stain-free gel in reducing conditions and

transferred to poly(vinylidene difluoride) membrane by Trans-Blot Turbo transfer system. To prevent nonspecific reactions from occurring, membranes were then blocked with 5% dry milk in 0.1% Tween 20 in Tris-buffered saline (TBST) for 1 h at RT, after which they were incubated overnight at 4 °C in a shaker with primary antibodies in blocking buffer overnight. On the next day, the membranes were washed with TBST and incubated with blocking buffer containing HRP-linked secondary antibody for 2 h at RT. Detection of secondary antibodies was done using a chemiluminescent substrate utilizing ChemiDoc XRS+ imaging System (Bio-Rad Laboratories, Hercules, CA, USA). For quantification, the optical densities of the immunoreactive protein bands were analysed using the ImageJ software (https://imagej.net/Downloads). The optical densities were first normalized to the corresponding loading control (GAPDH or β-actin) and then to the concurrent control on the same membrane. The experiments were replicated three times with two wells per condition in each experiment.

Serine/threonine kinome profiling

The Ser/Thr kinase (STK) profile of HMI-1a3 in Colo205 was determined by PamStation12 and STK PamChips (PamGene, s-Hertogenbosch, the Netherlands). The fluorescent platform measures phosphorylation of specific substrate peptides embedded on multiplex chip arrays by active kinases in the sample in the presence of ATP. Each array displays 144 immobilized phosphorylatable peptides of 15 amino acids, which correspond to known or reputed phosphorylation sites of human proteins derived from the literature and correlated with one or several upstream kinases.

The STK activity profiling was conducted according to manufacturer's standard protocol using reagents from Pamgene. The cells were grown on six-well plates and exposed to the compounds for 30 min or 2 h. After removal of the medium from the plate, the cells were washed with ice-cold PBS and lysed on ice with M-PER Mammalian Protein Extraction Reagent supplemented with Halt Phosphatase and Halt Protease inhibitor cocktails (all from Thermo Fisher Scientific, Paisley, UK). The lysate was centrifuged at 16,000 g for 15 min at

4 °C, and the supernatant immediately flash-frozen in liquid nitrogen, followed by storage at −80 °C. Total protein levels were determined by Bradford assay and the STK Basic Mix was composed of 1µg of the lysate, 4 µL 10 x protein reaction buffer, 0.4 µL of 100 x bovine serum albumin, 4.0 µL of 4 mM ATP, 0.46 µL STK antibody mix. Total volume of the STK Basic Mix was adjusted to 40 µL by adding distilled water. The detection mix consisted of 3 µL of 10 x antibody buffer, 0.4 µL fluorescein isothiocyanate (FITC) labelled STK antibody and 26.6 µL distilled water. The fluorescence was detected using a CCD camera and signals were integrated into one single value for each peptide with software-based image analysis. Raw image analysis was conducted using Evolve2 (Pamgene) software, with comparative analysis done in BioNavigator Analysis software (Pamgene). The mean phosphorylation intensities (following background correction) of each p-Ser/Thr peptide were normalized to the corresponding mean signal intensity of DMSO control treatment and expressed as log_2 fold-change ratio (LFC). Experiments were performed in biological triplicates.

High-content analysis

For HCA of proliferation and caspase activation, the staining, imaging and analysing of cells was done as described previously (Karhu et al., 2018). The cells were treated with the test compounds for 24 h and 10 µM BrdU was added to the culture medium for the last 1 h prior to fixation with 4% paraformaldehyde (PFA) for 15 min at RT. Immunofluorescence staining was done at RT as follows. The cells were permeabilised with 0.1% Triton X-100 for 10 min. DNA hydrolysis was done with 2 M hydrochloric acid for 30 min and subsequent neutralization with 0.1 M sodium borate (pH 8.5) for 30 min. After a 45-min blocking with 4% FBS in PBS, the cells were incubated with anti-BrdU antibody (1:250) for 1 h followed by 3 × 5 min washes with PBS and a 45-min incubation with Alexa Fluor 647-conjugated secondary antibody (1:200) and DAPI (5 µg/ml) for 45 min. For the analysis of caspase activation, the cells were treated with the compounds for 4 h and then incubated with 5 µM CellEvent™ Caspase-3/7 Green Detection Reagent solution in PBS with 5% FBS for 50 min before fixation.

The samples were imaged with ImageXpress Nano high content imaging system (Molecular Devices, Winnersh, UK). Sixteen images per well were collected using a 10x objective to analyse >100 cells from each well. The images were analysed with the MetaXpress software, as follows: the nuclei were first identified based on DNA staining (DAPI). The nuclear fluorescence intensity at 647 nm was quantified as a measure of BrdU, and the nuclear fluorescence intensity at 488 nm was quantified as a measure of caspase 3/7 activity.

Statistics

Statistical analyses and IC_{50} value calculations were performed using GraphPad Prism (version 7.04) software for Windows (GraphPad Software, La Jolla, CA, USA, www.graphpad.com). Control refers to incubation with vehicle (0.1% DMSO). N refers to the number of independent experiments, for which two or more parallel samples (technical replicates) were averaged to produce N=1. Data is presented as the mean of independent experiments, the number of which is indicated in the corresponding figure legends.

Results

HMI-1a3 decreases the viability of colorectal cancer cell lines concentration-dependently but in a PKC independent manner

Caco-2, Colo205, and HT-29 cells, were treated with HMI-1a3 at concentrations ranging from 0.1 - 20 µM for 24 h and cell viability was analysed with the MTT assay (Figure 1A). HMI-1a3 decreased the viability of all the studied cell lines in a concentration-dependent manner after 24 h exposure. IC_{50} values were 2.9 µM, 0.69 µM and 0.64 µM for Caco2, Colo205 and HT29 cell lines, respectively. HMI-1a3 did not induce cell membrane damage as determined by the LDH activity in cell culture medium (Supplementary Tables S1, S2 and S3). Simultaneous treatment with the pan-PKC inhibitor Gö6983 (1µM) did not attenuate the HMI-1a3-induced CRC cell viability reduction (Figure 1B).

HMI-1a3 induces anti-proliferative and pro-apoptotic effects in colorectal cancer cell lines

HCA and PARP-immunoblotting were used to study whether the decreased cell viability is due to the effects of HMI-1a3 on the proliferation and apoptosis of the CRC cell lines (Figure 2 and Supplementary Figure S1). The potent PKC activator PMA was used to assess the possible role of PKC and staurosporine, a widely used inducer of apoptosis, as a positive control. On Caco2 cells HMI-1a3 did not have any clear effect on caspase 3/7 activity on after 24 h exposure, whereas on Colo205 and HT29 cells 20 µM HMI-1a3 increased the proportion of caspase positive cells (Figure 2B). HMI-1a3 20µM decreased the percentage of BrdU positive cells significantly in all cell lines studied (Figure 2C). Both PMA and staurosporine had inconsistent effects in different cell lines (Figure 2).

Since the number of caspase 3/7 positive cells was very low, we hypothesised that the treatments or the fixing procedure may have detached dead cells and thus reduced the number of cells in the HCA results (Figure 2B, D). To abolish the uncertainty, we decided to verify the apoptosis by detecting the PARP cleavage with immunoblotting where a clear

increase in the PARP cleavage in all the cell lines tested was observed (Supplementary Figure S1). The CRC cells did not show senescent-like morphology or altered E2F1 or p21 expression (Supplementary Figure S2), ruling out the senescence as a cause of reduced viability in response to HMI-1a3, as previously observed in DU145 and PC3 prostate cancer cells (Jäntti et al., 2018).

Early effects of HMI-1a3 on kinase activity of Colo205 cells

Since the HMI-1a3-induced decline in CRC cell viability was PKC independent, we sought to profile the effect of HMI-1a3 on the activity of STK on Colo205 cells following 30 minute and 2 hour exposures, using PamStation 12. We hypothesised that the top ranked kinases would represent the most relevant non-PKC mediators of HMI-1a3 anticancer activity. Kinase profiling revealed increased activation of several kinases, whereas no decrease of kinase activity was observed (Supplementary Figures S3 and S4). Kinases were ranked based on median final score, and a higher specificity score indicates a higher likelihood of the corresponding kinase contributing to the observed phosphorylation changes (Tables 1 and 2). The changes in the kinase activity, however, were quite modest in both time points compared to control.

The obtained kinase profile was reflected on literature to delineate the potential pathways of the observed effects of HMI-1a3 on cancer cell viability. Extracellular signal-regulated kinase 7 (ERK7), which was activated after a 30 min HMI-1a3 treatment has been shown to serve both as a proto-oncogene and as a tumour suppressor (Lau & Xu, 2018). Calcium/calmodulin-dependent protein kinase type 2 (CaMK 2) (Chen et al., 2017) and cyclin-dependent kinase 14 (CDK14) (Zhou et al., 2014) have been shown to be over-expressed in human colon cancer and contribute to invasiveness. The most upregulated kinases were different after 2 hours compared to 30 minutes (Table 2, Supplementary Figure S4) and there was no clear correlation or trend between the time points. One of the most activated kinases after the 2 hour time point was cyclin-dependent kinase-like 2 (CDKL2). Downregulation or loss of CDKL2 has been associated with several cancer cell types,

including colorectal cancer and its overexpression suppresses cells growth and invasion (Fang et al., 2018). This information suggests that CDKL2 activation by HMI-1a3 could mediate the observed decrease in viability in colorectal cancer cells. The other three most activated kinases, intestinal cell kinase (ICK) (Whitworth et al., 2012), alpha-protein kinase (AlphaK1) (Chen et al., 2019) and cyclin-dependent kinase-like 5 (CDKL5) (Jiang et al., 2019), are associated with tumour growth and aggressiveness. Being among the most activated kinases, according to the upstream kinase interpretation, cyclic AMP-dependent protein kinase A (PKA) and cyclic GMP-dependent protein kinase G (PKG) also demonstrated high specificity score or consistency in activity on both time points (Tables 1 and 2, Supplementary Figures S3 and S4).

Unravelling the mediators of HMI-1a3-induced effects in Colo205 cells

HMI-1a3 has been designed to bind PKC and in addition to PKCα and –δ (Boije af Gennäs et al., 2009) it has been demonstrated to bind to β2-chimaerin, protein kinase D1 (PKD1) and myotonic dystrophy kinase–related CDC42-binding kinase-α (MRCKα) (Talman et al., 2014), all of which also contain the C1 structure. However, the effect of HMI-1a3 on CRC viability was not antagonized by the pan-PKC inhibitor Gö6983 (1 µM), the cPKC and PKD1 inhibitor Gö6976 (2 µM) nor by the inhibitors of main MAPK families MEK1/2, JNK and p38α/p38β (U0126; 10 µM, SP600125; 10 µM and SB20358; 5 µM respectively), that are well-known downstream mediators of PKC activation (Figure 3A and B). Therefore, we next tested a set of kinase inhibitors, based on the STK profiling to find the possible mediators of the observed HMI-1a3 induced effects.

The PKG, PKC and PKA inhibitor (K_i values 0.23, 4 and > 10 µM respectively) KT5823 reversed the HMI-1a3 induced decrease in cell viability at 10 µM concentration (Figure 3C, D, E). The more specific inhibitors of PKA KT5720 (5 µM) and cAMPS-Rp (100 µM) attenuated the effects of HMI-1a3 to some extent, yet not as strongly as KT5823, whereas the PKG inhibitor (Rp-8-pCPT-cGMPS; 250 µM) did not antagonise the observed effects of HMI-1a3 (Figure 3C, D). Also the CaMK 2 inhibitor KN93 (9 µM) seemed to block the viability

decreasing effect of 1 µM HMI-1a3, but not that of 20 µM HMI-1a3 (Figure 3C, D). Phospholipase C inhibitor U73122 (5 µM) did not mitigate the effect of HMI-1a3. Based on these findings KT5823, KT5720 and KN93 were chosen for a more profound concentration-response experiment, where it was shown that KT5823 and KT5720 inhibited the effect of HMI-1a3 on cell viability significantly, whereas KN93 seemed to increase the metabolic activity itself making it difficult to distinguish its possible HMI-1a3 inhibiting effect (Figure 3E, F, G).

Sir Philip Cohen's group showed in their kinase inhibitor screening (Bain et al., 2003) that instead of PKG, PKC or PKA, KT5823 inhibits p38-activated protein kinase (PRAK) and glycogen synthase kinase 3β (GSK-3β). They also suggested that there might be significant inter-batch differences explaining the lack of PKG inhibiting properties. Because of this, we studied the effects of PRAK and GSK-3 inhibitors (PF3644022; 250 µM and CHIR99021; 12 µM respectively), but they did not affect the decrease in cell viability (Figure 3C, D). Furthermore, we did not observe any inter-batch differences between compound batches used in our assays.

In order to characterise the possible role of PKA and PKG, the phosphorylation of VASP after 30 minutes was investigated using immunoblotting. Since several phosphorylation sites of VASP have been identified, we studied both the major PKA phosphorylation site Ser157 as well as the major PKG phosphorylation site Ser239 (Smolenski et al., 1998). A 30 minute exposure to 1 and 20µM HMI-1a3 increased the phosphorylation of the VASP Ser157, indicating that HMI-1a3 treatment indeed activates PKA in Colo205 cells (Figure 4). An opposite effect was observed on the phosphorylation of VASP at Ser239. KT5823 inhibited HMI-1a3 induced VASP phosphorylation at Ser157.

Discussion

Even though PKC has been generally considered as an oncogenic kinase, several studies have demonstrated that loss of PKC activity is often associated with cancer. In these cases PKC isoforms function as tumour suppressors rather than promoters (Newton, 2018). Consistent with these findings, the development of PKC activators not inducing downregulation of PKC protein levels should be the basis for a potential new mechanism of action for an anti-cancer drug (Bessa et al., 2018; Boije af Gennäs et al., 2009; Oliva et al., 2008).

In our previous studies, we showed that the derivative of isophthalic acid, HMI-1a3, binds to the C1 domain and activates PKCs without inducing downregulation (Boije af Gennäs et al., 2009). HMI-1a3 has been shown to inhibit the proliferation of HeLa cervical cancer cells (Talman et al., 2011) and DU145, PC3 and LNCaP prostate cancer cells (Jäntti et al., 2018). HMI-1a3 induced apoptosis in LNCaP cells and senescence in DU145 and PC3 cells. In HeLa, PC3 and DU145 cells, the pan-PKC inhibitor Gö6983 did not attenuate the effects of HMI-1a3, whereas in LNCaP cells its effect seems to be mediated by PKC (Jäntti et al., 2018; Talman et al., 2014; Talman et al., 2011).

In the current study, we characterized the effects of HMI-1a3 on colorectal cancer cells *in vitro*, since it has been previously suggested that PKC acts as a tumour suppressor in colorectal cancer (Doi et al., 1994; Dowling et al., 2016; Goldstein et al., 1995; Lee et al., 2010). HMI-1a3 decreased the viability and induced apoptosis in all tested CRC cell lines; however, the observed effects were not attenuated with the PKC inhibitors Gö6983 or Gö6976. Since it seemed that the effects of isophthalic acid derivative HMI-1a3 were not mediated by PKC nor by the downstream mediators of PKC signalling, we investigated its mechanism-of-action utilising a Pamgene serine/threonine kinome-profiling assay. It is important to acknowledge that the kinome profile relies on literature and databases and it is an interpretation from the phosphopeptide read-out. The profile of the early effects of HMI-1a3 did not include any of the known C1 domain containing proteins (Griner & Kazanietz,

17

2007; Kazanietz, 2002; Talman et al., 2014) nor were there any clear trends between the two time points. The results, however, suggested that PKA and PKG play a role, even though cAMP/PKA or cGMP/PKG related kinases were not among the top hit kinases in the latter time point. We subsequently showed that a non-specific PKG inhibitor KT5823 and two different PKA inhibitors attenuated the viability decreasing effects of HMI-1a3. More detailed investigation revealed that HMI-1a3 increased the phosphorylation of VASP at Ser157, while surprisingly decreased the phosphorylation at Ser239. Ser157 is a preferred phosphorylation site for PKA and Ser239 is the preferential phosphorylation site for PKG, thus this finding supports a preferential involvement of cAMP–PKA pathway in the effects of HMI-1a3. In some cases, VASP Ser157 is also phosphorylated by PKC (Chitaley et al., 2004) and PKD1 and -2 (Doppler et al., 2015; Doppler et al., 2013), but here the effect was shown to be PKA mediated.

Activation of cAMP-PKA signalling and phosphorylation of VASP Ser157 has tumour-suppressive and -promoting effects depending on the tumour types and tissue of origin (Ali et al., 2021; Zhang et al., 2020). Activation of the cAMP-PKA signalling with the cAMP analogue 8-Cl-cAMP has been demonstrated to inhibit the growth of CRC, breast cancer, lung cancer, and leukaemia *in vitro* and *in vivo* (Zhang et al., 2020). These results are consistent with our current finding that the anticancer activity of HMI-1a3 was inhibited by the cAMP analogue cAMPS-Rp, which inhibits PKA. The significance of VASP Ser157 phosphorylation in the regulation of cancer cell signalling is controversial. The anticancer drug Imatinib restores the phosphorylation of VASP Ser157 and decreases VASP and BCR–ABL interaction in Imatinib responsive chronic myelogenous leukaemia (Bernusso et al., 2015). In prostate cancer cells, Ser157 phosphorylation of VASP correlates with cell motility and has been suggested to be a marker for metastatic progression potential (Hasegawa et al., 2008). In a recent study, VASP Ser157 phosphorylation was associated with enhanced colon cancer cell clonogenicity and migration in vitro, and growth into tumours in nude mice (Ali et al., 2021). However, phosphorylation of VASP Ser239 phosphorylation had an

opposite effect. Our results with cAMP analogues and HMI-1a3 support a hypothesis that there is a certain balance in the phosphorylation of VASP Ser157 and VASP Ser239, which contribute to the tumour suppressing effect of PKA activation. This may explain the differential findings of tumour cell-line suppressive effects of PKA-signalling in some but not all experimental settings.

Previously established antiproliferative and pro-apoptotic effects of compounds that modulate cAMP/PKA signalling suggest a potential mechanisms of action by which HMI-1a3-induces its PKA mediated anticancer effects. These include for example adenylyl cyclase activation, though which forskolin has demonstrated anticancer potential via PKA activation (Follin-Arbelet et al., 2015). Another hypothetical mechanism of action is that HMI-1a3 could act as an inhibitor of phosphodiesterases (PDEs), which control the amount of cAMP. PDE inhibitors specific for cAMP have been suggested to possess cancer drug candidate potential (Peng et al., 2018). However, the contribution of other proteins containing a DAG-responsive C1 domain in the effects of HMI-1a3 cannot be excluded (Figure 5).

When interpreting studies only utilising cell lines, it is important to keep in mind that in two-dimensional models, the cell interactions do not accurately mimic the situation on the tissue level, where several factors, such as tumour microenvironment, play a significant role (Fitzgerald et al., 2015; Peddareddigari et al., 2010). Thus, in further *in vitro* studies primary cancer cells as well as 3D spheroid models could better simulate clinical circumstances. An additional limitation of the current study is that the small molecule compounds used as pharmacological tools may also target other kinases. Alternatively, PKA knockdown or overexpression could have been used to confirm the observed effects; however compensatory expression changes and redundant roles of various kinases also complicates the interpretation of such studies.

In conclusion, our study identified PKA activation as a new-anti-cancer mechanism of action for the PKC-targeted isophthalate derivative HMI-1a3 (Figure 5). The mechanism by which HMI-1a3 activates PKA remains to be clarified in further studies. Furthermore, additional

investigation is required to characterise the role of cAMP-PKA signalling in the other PKC-independent effects we have previously reported.

Acknowledgements

Author Contributions

Participated in research design: Tarvainen, Jäntti, Tuominen and Talman

Conducted experiments: Tarvainen and Nunn

Performed data analysis: Tarvainen and Nunn

Contributed to the writing of the manuscript: Tarvainen, Jäntti, Tuominen and Talman

Conflicts of Interest

No author has an actual or perceived conflict of interest with the contents of this article.

References

Ali M, Zuzga DS, & Pitari GM (2021). Differential Ser phosphorylation of vasodilator-stimulated phosphoprotein regulates colon tumor formation and growth. Life Sci 264: 118671.

Antal CE, Hudson AM, Kang E, Zanca C, Wirth C, Stephenson NL, Trotter EW, Gallegos LL, Miller CJ, Fumari FB, Hunter T, Brognard J, & Newton AC (2015). Cancer-Associated Protein Kinase C Mutations Reveal Kinase's Role as Tumor Suppressor. Cell 160: 489-502.

Bain J, McLauchlan H, Elliott M, & Cohen P (2003). The specificities of protein kinase inhibitors: an update. Biochem J 371: 199-204.

Bernusso VA, Machado-Neto JA, Pericole FV, Vieira KP, Duarte AS, Traina F, Hansen MD, Olalla Saad ST, & Barcellos KS (2015). Imatinib restores VASP activity and its interaction with Zyxin in BCR-ABL leukemic cells. Biochim Biophys Acta 1853: 388-395.

Bessa C, Soares J, Raimundo L, Loureiro JB, Gomes C, Reis F, Soares ML, Santos D, Dureja C, Chaudhuri SR, Lopez-Haber C, Kazanietz MG, Goncalves J, Simoes MF, Rijo P, & Saraiva L (2018). Discovery of a small-molecule protein kinase Cdelta-selective activator with promising application in colon cancer therapy. Cell Death Dis 9: 23.

Boije af Gennäs G, Talman V, Aitio O, Ekokoski E, Finel M, Tuominen RK, & Yli-Kauhaluoma J (2009). Design, synthesis, and biological activity of isophthalic acid derivatives targeted to the C1 domain of protein kinase C. J Med Chem 52: 3969-3981.

Bray F, Ferlay J, Soerjomataram I, Siegel RL, Torre LA, & Jemal A (2018). Global cancer statistics 2018: GLOBOCAN estimates of incidence and mortality worldwide for 36 cancers in 185 countries. Ca-Cancer J Clin 68: 394-424.

Bray F, & Soerjomataram I (2015). The Changing Global Burden of Cancer: Transitions in Human Development and Implications for Cancer Prevention and Control. In Cancer: Disease Control Priorities, Third Edition (Volume 3). eds Gelband H., Jha P., Sankaranarayanan R., & Horton S.: Washington (DC).

Brenner H, Bouvier AM, Foschi R, Hackl M, Larsen IK, Lemmens V, Mangone L, Francisci S, & Group EW (2012). Progress in colorectal cancer survival in Europe from the late 1980s to the early 21st century: the EUROCARE study. Int J Cancer 131: 1649-1658.

Chen PK, Hua CH, Hsu HT, Kuo TM, Chung CM, Lee CP, Tsai MH, Yeh KT, & Ko YC (2019). ALPK1 Expression Is Associated with Lymph Node Metastasis and Tumor Growth in Oral Squamous Cell Carcinoma Patients. Am J Pathol 189**:** 190-199.

Chen W, An P, Quan XJ, Zhang J, Zhou ZY, Zou LP, & Luo HS (2017). Ca(2+)/calmodulin-dependent protein kinase II regulates colon cancer proliferation and migration via ERK1/2 and p38 pathways. World J Gastroenterol 23**:** 6111-6118.

Chitaley K, Chen L, Galler A, Walter U, Daum G, & Clowes AW (2004). Vasodilator-stimulated phosphoprotein is a substrate for protein kinase C. FEBS Lett 556**:** 211-215.

Choi PM, Tchouwong KM, & Weinstein IB (1990). Overexpression of Protein-Kinase-C in Ht29 Colon Cancer-Cells Causes Growth-Inhibition and Tumor Suppression. Molecular and Cellular Biology 10**:** 4650-4657.

Cohen P, Cross D, & Janne PA (2021). Kinase drug discovery 20 years after imatinib: progress and future directions. Nat Rev Drug Discov 20**:** 551-569.

Craven PA, & DeRubertis FR (1994). Loss of protein kinase C delta isozyme immunoreactivity in human adenocarcinomas. Dig Dis Sci 39**:** 481-489.

Doi S, Goldstein D, Hug H, & Weinstein IB (1994). Expression of multiple isoforms of protein kinase C in normal human colon mucosa and colon tumors and decreased levels of protein kinase C beta and eta mRNAs in the tumors. Mol Carcinog 11**:** 197-203.

Doppler H, Bastea L, Borges S, Geiger X, & Storz P (2015). The phosphorylation status of VASP at serine 322 can be predictive for aggressiveness of invasive ductal carcinoma. Oncotarget 6**:** 29740-29752.

Doppler HR, Bastea LI, Lewis-Tuffin LJ, Anastasiadis PZ, & Storz P (2013). Protein kinase D1-mediated phosphorylations regulate vasodilator-stimulated phosphoprotein (VASP) localization and cell migration. J Biol Chem 288**:** 24382-24393.

Dowling CM, Phelan J, Callender JA, Cathcart MC, Mehigan B, McCormick P, Dalton T, Coffey JC, Newton AC, O'Sullivan J, & Kiely PA (2016). Protein kinase C beta II suppresses colorectal cancer by regulating IGF-1 mediated cell survival. Oncotarget 7**:** 20919-20933.

Fang CL, Uen YH, Chen HK, Hseu YC, Lin CC, Hung ST, Sun DP, & Lin KY (2018). Loss of cyclin-dependent kinase-like 2 predicts poor prognosis in gastric cancer, and its overexpression suppresses cells growth and invasion. Cancer Med 7**:** 2993-3002.

FDA (2021). Available from www.fda.gov. [Accessed: 20.8.2021].

Fitzgerald KA, Malhotra M, Curtin CM, FJ OB, & CM OD (2015). Life in 3D is never flat: 3D models to optimise drug delivery. J Control Release 215**:** 39-54.

Follin-Arbelet V, Misund K, Naderi EH, Ugland H, Sundan A, & Blomhoff HK (2015). The natural compound forskolin synergizes with dexamethasone to induce cell death in myeloma cells via BIM. Sci Rep 5**:** 13001.

Goldstein DR, Cacace AM, & Weinstein IB (1995). Overexpression of protein kinase C beta 1 in the SW480 colon cancer cell line causes growth suppression. Carcinogenesis 16**:** 1121-1126.

Griner EM, & Kazanietz MG (2007). Protein kinase C and other diacylglycerol effectors in cancer. Nat Rev Cancer 7**:** 281-294.

Hasegawa Y, Murph M, Yu S, Tigyi G, & Mills GB (2008). Lysophosphatidic acid (LPA)-induced vasodilator-stimulated phosphoprotein mediates lamellipodia formation to initiate motility in PC-3 prostate cancer cells. Mol Oncol 2**:** 54-69.

Jiang Z, Gong T, & Wei H (2019). CDKL5 promotes proliferation, migration, and chemotherapeutic drug resistance of glioma cells via activation of the PI3K/AKT signaling pathway. Febs Open Bio.

Jäntti MH, Talman V, Räsänen K, Tarvainen I, Koistinen H, & Tuominen RK (2018). Anticancer activity of the protein kinase C modulator HMI-1a3 in 2D and 3D cell culture models of androgen-responsive and androgen-unresponsive prostate cancer. Febs Open Bio 8**:** 817-828.

Karhu ST, Ruskoaho H, & Talman V (2021). Distinct Regulation of Cardiac Fibroblast Proliferation and Transdifferentiation by Classical and Novel Protein Kinase C Isoforms: Possible Implications for New Antifibrotic Therapies. Mol Pharmacol 99**:** 104-113.

Karhu ST, Välimäki MJ, Jumppanen M, Kinnunen SM, Pohjolainen L, Leigh RS, Auno S, Foldes G, Boije Af Gennäs G, Yli-Kauhaluoma J, Ruskoaho H, & Talman V (2018). Stem cells are the most sensitive screening tool to identify toxicity of GATA4-targeted novel small-molecule compounds. Arch Toxicol 92**:** 2897-2911.

Kazanietz MG (2002). Novel "nonkinase" phorbol ester receptors: the C1 domain connection. Mol Pharmacol 61**:** 759-767.

Kisslov L, Hadad N, Rosengraten M, & Levy R (2012). HT-29 human colon cancer cell proliferation is regulated by cytosolic phospholipase A(2)alpha dependent PGE(2)via both PKA and PKB pathways. Biochim Biophys Acta 1821**:** 1224-1234.

Lau ATY, & Xu YM (2018). Regulation of human mitogen-activated protein kinase 15 (extracellular signal-regulated kinase 7/8) and its functions: A recent update. J Cell Physiol 234**:** 75-88.

Lee JM, Kim IS, Kim H, Lee JS, Kim K, Yim HY, Jeong J, Kim JH, Kim JY, Lee H, Seo SB, Kim H, Rosenfeld MG, Kim KI, & Baek SH (2010). RORalpha attenuates Wnt/beta-catenin signaling by PKCalpha-dependent phosphorylation in colon cancer. Mol Cell 37**:** 183-195.

Newton AC (2018). Protein kinase C as a tumor suppressor. Semin Cancer Biol 48**:** 18-26.

Oliva JL, Caino MC, Senderowicz AM, & Kazanietz MG (2008). S-Phase-specific activation of PKC alpha induces senescence in non-small cell lung cancer cells. J Biol Chem 283**:** 5466-5476.

Ouaret D, & Larsen AK (2014). Protein kinase C beta inhibition by enzastaurin leads to mitotic missegregation and preferential cytotoxicity toward colorectal cancer cells with chromosomal instability (CIN). Cell Cycle 13**:** 2697-2706.

Peddareddigari VG, Wang D, & Dubois RN (2010). The tumor microenvironment in colorectal carcinogenesis. Cancer Microenviron 3**:** 149-166.

Peng T, Gong J, Jin Y, Zhou Y, Tong R, Wei X, Bai L, & Shi J (2018). Inhibitors of phosphodiesterase as cancer therapeutics. Eur J Med Chem 150**:** 742-756.

Pongracz J, Clark P, Neoptolemos JP, & Lord JM (1995). Expression of protein kinase C isoenzymes in colorectal cancer tissue and their differential activation by different bile acids. Int J Cancer 61**:** 35-39.

Roskoski R, Jr. (2015). A historical overview of protein kinases and their targeted small molecule inhibitors. Pharmacol Res 100**:** 1-23.

Sarajärvi T, Jäntti M, Paldanius KMA, Natunen T, Wu JC, Mäkinen P, Tarvainen I, Tuominen RK, Talman V, & Hiltunen M (2018). Protein kinase C -activating isophthalate derivatives mitigate Alzheimer's disease-related cellular alterations. Neuropharmacology 141**:** 76-88.

Smolenski A, Bachmann C, Reinhard K, Honig-Liedl P, Jarchau T, Hoschuetzky H, & Walter U (1998). Analysis and regulation of vasodilator-stimulated phosphoprotein serine 239 phosphorylation in vitro and in intact cells using a phosphospecific monoclonal antibody. J Biol Chem 273**:** 20029-20035.

Spindler KL, Lindebjerg J, Lahn M, Kjaer-Frifeldt S, & Jakobsen A (2009). Protein kinase C-beta II (PKC-beta II) expression in patients with colorectal cancer. Int J Colorectal Dis 24**:** 641-645.

Suga K, Sugimoto I, Ito H, & Hashimoto E (1998). Down-regulation of protein kinase C-alpha detected in human colorectal cancer. Biochem Mol Biol Int 44**:** 523-528.

Talman V, Gateva G, Ahti M, Ekokoski E, Lappalainen P, & Tuominen RK (2014). Evidence for a role of MRCK in mediating HeLa cell elongation induced by the C1 domain ligand HMI-1a3. Eur J Pharm Sci 55**:** 46-57.

Talman V, Tuominen RK, Boije af Gennäs G, Yli-Kauhaluoma J, & Ekokoski E (2011). C1 Domain-targeted isophthalate derivatives induce cell elongation and cell cycle arrest in HeLa cells. PLoS One 6**:** e20053.

Tarvainen I, Zimmermann T, Heinonen P, Jantti MH, Yli-Kauhaluoma J, Talman V, Franzyk H, Tuominen RK, & Christensen SB (2020). Missing Selectivity of Targeted 4beta-Phorbol Prodrugs Expected to be Potential Chemotherapeutics. ACS Med Chem Lett 11**:** 671-677.

Whitworth H, Bhadel S, Ivey M, Conaway M, Spencer A, Hernan R, Holemon H, & Gioeli D (2012). Identification of kinases regulating prostate cancer cell growth using an RNAi phenotypic screen. PLoS One 7**:** e38950.

Zhang H, Kong Q, Wang J, Jiang Y, & Hua H (2020). Complex roles of cAMP-PKA-CREB signaling in cancer. Exp Hematol Oncol 9**:** 32.

Zhao Y, Wang Y, Zhao J, Zhang Z, Jin M, Zhou F, Jin C, Zhang J, Xing J, Wang N, He X, & Ren T (2021). PDE2 Inhibits PKA-Mediated Phosphorylation of TFAM to Promote Mitochondrial Ca(2+)-Induced Colorectal Cancer Growth. Front Oncol 11**:** 663778.

Zhou Y, Rideout WM, 3rd, Bressel A, Yalavarthi S, Zi T, Potz D, Farlow S, Brodeur J, Monti A, Reddipalli S, Xiao Q, Bottega S, Feng B, Chiu MI, Bosenberg M, & Heyer J (2014). Spontaneous genomic alterations in a chimeric model of colorectal cancer enable metastasis and guide effective combinatorial therapy. PLoS One 9**:** e105886.

Footnotes

Figure legends

Figure 1. Effects of HMI-1a3 on CRC cell line viability. (A) HMI-1a3 decreased the viability of Caco-2, Colo205 and HT29 CRC cells concentration-dependently. (B) The effect was not reversed by PKC inhibitor Gö6983 (1 µM). Cell viability was measured in the MTT assay after 24 h exposure with HMI-1a3. The data are presented as mean (A) ± SEM and (B) +SEM (N = 3; *P < 0.05; **P < 0.01 vs control, ANOVA followed by Dunnett's test).

Figure 2. Effects of HMI-1a3 on cell proliferation and caspase activation in Caco2, Colo205 and HT29 CRC cell lines. After a 24-h compound incubation, the cells were incubated with BrdU (1 h) and detection reagent for activated caspase-3/7 (50 min) (green) and subsequently fixed and stained for DNA (DAPI) (blue) and BrdU (magenta). (A) Representative images from each cell line and treatment are shown. Individual colour channels were adjusted to enhance brightness and contrast for all representative images. Normalised number of cells positive for fluorescent caspase 3/7 activity reporter (B), quantification of the proportion of cells positive for BrdU (C) and normalised number of cells (D) are presented as mean + SEM (N = 3; *P < 0.05; **P < 0.01 vs ctrl, ANOVA followed by Dunnet's test).

Figure 3. Effect of different inhibitors on the HMI-1a3 compromised viability of Colo205 colorectal cancer cells. (A, B) PKC inhibitors Gö6983 and Gö6976, MEK1/2 inhibitor U0126, MAPK inhibitor SB203580 or JNK inhibitor SP600125 did not antagonise the effect of 1 µM (A) or 20 µM (B) HMI-1a3. PKG KT5823 (C, D, E), PKA inhibitors KT5720 and cAMPS-Rp (C, D, F) as well as CaM kinase II inhibitor KN93 (C, D, G) inhibited the effects of HMI-1a3 fully or partially, while the PKG inhibitor Rp-8-pCPT-cGMPS, MK2/PRAK inhibitor PF 3644022, GSK-3 inhibitor CHIR99021 or phospholipase C inhibitor U73122 did not (A, B). Cell viability was measured utilizing MTT assay. Data presented as mean + SEM. For A and

B N = 3; *P < 0.05; **P < 0.01; ***P < 0.001 vs HMI-1a3 treatment, ANOVA followed by Dunnett's test. For C, D, E, F and G N = 3; *P < 0.05; **P < 0.01; ***P < 0.001 vs. the corresponding HMI-1a3 treatment, Student's t-test.

Figure 4. HMI-1a3 increases the phosphorylation of VASP at serine 157, but not at serine 239 in Colo205 CRC cell line after 30 minute treatment. (A) Representative Western blots and quantifications of the proportion of (B) phosphorylated VASP (Ser 157) and (C) VASP (Ser 239) in response to HMI-1a3 and KT5823. Data are presented as mean + SEM (N = 3; *P < 0.05; **P < 0.01 vs ctrl, ANOVA followed by Dunnet's test).

Figure 5. Schematic representation of known and newly recognised targets of HMI-1a3 as well as the main findings of this study.

Tables

Table 1: Ten top ranked kinases after 30 minute exposure to 20 μM of HMI-1a3 compared to control according to the upstream kinase analysis.

Uniprot ID	Kinase name	Median Final Score	Specificity score
Q8TD08	Mitogen-activated protein kinase 15 (MAPK15/ERK7)	2.7	1.7
P17612	Protein kinase A (PKAα)	2.5	1.8
Q13535	ataxia telangiectasia and Rad3-related protein (ATR)	2.0	1.0
Q9UQM7	Calcium/calmodulin-dependent protein kinase type 2 subunit α (CaMK2α)	2.0	1.3
Q00526	Cyclin-dependent kinase 3 (CDK3)	1.9	0.9
Q13976	cGMP-dependent protein kinase 1 (PKG1)	1.9	1.2
P11309	Serine/threonine-protein kinase pim-1 (Pim1)	1.9	1.2
O94921	Cyclin-dependent kinase 14 (CDK14)	1.8	1.1
Q13237	cGMP-dependent protein kinase 2 (PKG2)	1.7	0.9
P51817	cAMP-dependent protein kinase catalytic subunit PRKX (PRKX)	1.6	1.0

Table 2. Ten top ranked kinases after 2 hour exposure to 20 µM of HMI-1a3 compared to control according to the upstream kinase analysis.

Uniprot ID	Kinase name	Median Final Score	Specificity score
Q9UPZ9	Intestinal cell kinase (ICK)	2.4	2.0
Q92772	Cyclin-dependent kinase-like 2 (CDKL2)	2.3	1.9
Q96L96	Alpha-protein kinase (AlphaK1)	2.3	1.8
O76039	Cyclin-dependent kinase-like 5 (CDKL5)	2.1	1.7
Q14164	Inhibitor of nuclear factor kappa-B kinase subunit epsilon (IKKε)	1.9	1.6
Q96S38	Ribosomal protein S6 kinase delta-1 (RSKL1)	1.6	1.2
Q9UHD2	TANK-binding kinase 1 (TBK1)	1.6	1.3
P49840	Glycogen synthase kinase-3 alpha (GSK3α)	1.6	0.9
P17252	Protein kinase C alpha (PKCα)	1.6	1.2
O15530	3-phosphoinositide-dependent protein kinase 1 (PDK1)	1.5	1.0